Spectral function and photoemission spectra in antiferromagnetically correlated metals

Arno P. Kampf, J. R. Schrieffer

Spectral function and photoemission spectra in antiferromagnetically correlated metals

A. P. Kampf and J. R. Schrieffer*

Advanced Studies Program in High Temperature Superconductivity Theory, Los Alamos National Laboratory,
Los Alamos, New Mexico 87545

Antiferromagnetic spin fluctuations in a two-dimensional metal, such as doped high-T_c superconductors, lead to a pseudogap in the electronic spectrum. In the spectral function weight is shifted from the single quasiparticle peak of the Fermi-liquid regime to the incoherent particle and hole backgrounds, which evolve into the upper and lower Mott-Hubbard bands of the antiferromagnetic insulator. Precursors of these split bands show up as "shadow bands" in angle-resolved photoemission spectra.

I. INTRODUCTION

A striking feature of high-temperature oxide superconductors is the proximity of antiferromagnetism and superconductivity in nearby regions of the phase diagram with different doping concentrations. The superconducting compounds show metallic behavior in their normal state with short- or intermediate-range antiferromagnetic (AF) spin correlations that persist into the superconducting state. Taking the point of view that the effective (screened and correlated) on-site electron-electron Coulomb repulsion U in these materials is smaller than the bandwidth, an appropriate starting point is to take the electrons as being itinerant. In this framework, antiferromagnetism is described as a spin-density wave (SDW), which arises, e.g., from the Fermi surface nesting of the half-filled two-dimensional square lattice with nearest-neighbor hopping. In the regime relevant for the superconducting cuprates with strong short-range AF spin fluctuations, the density of states near the Fermi energy is suppressed, leading to a pseudogap. With increasing spin-correlation length the pseudogap evolves into the SDW gap that extends over the entire Fermi surface and the system becomes an AF insulator.

Extending our previous analysis of the pseudogap,[1] in this paper we discuss the evolution of the one-particle spectral function from the Fermi-liquid regime to the case of intermediate-range antiferromagnetic order. The specific model that we consider is the single-band Hubbard model on a square lattice. Starting from the large doping limit with weak spin correlations, we can address two questions related to the evolution of antiferromagnetism as we move towards half-filling: (1) how do the antiferromagnetic spin fluctuations build up as reflected in the spin susceptibility $\chi(\mathbf{q},\omega)$. (2) Given a phenomenological form for χ, what are the consequences of the AF fluctuations for the fermionic single-particle spectrum. In this paper we focus on the latter question and explore how a model for $\chi(\mathbf{q},\omega)$ motivated by experiment leads to single-particle properties that are directly measurable by, e.g., photoemission and inverse photoemission experiments.

From neutron-scattering experiments on $La_{1.85}Sr_{0.15}CuO_4$ (Ref. 2) and $YBa_2Cu_3O_{6.5}$ (Ref. 3), as well as from NMR measurements,[4] the presence of antiferromagnetic spin fluctuations in these materials has been well established. We know that the magnetic structure factor

$$S(\mathbf{q},\omega)=\frac{1}{1-e^{-\beta\omega}}\mathrm{Im}\chi^{zz}(\mathbf{q},\omega)\qquad(1)$$

and the spin susceptibility χ^{zz} are peaked near the AF wave vector $\mathbf{Q}=(\pi,\pi)$. The inverse of the width of the peak is a direct measure of the spin-spin correlation length. The direct determination of the correlation length is complicated because in the superconducting samples the central peak at $\mathbf{Q}$ appears to be symmetrically split into two adjacent maxima[5] introducing some uncertainty for the actual peak width. The splitting may be either due to discommensurations leading to the formation of domains, in each of which the magnetic order is still commensurate with the underlying lattice or an incommensurate SDW.

Since this complication has little effect on our results we take $\chi(\mathbf{q},\omega)$ to be peaked at $\mathbf{Q}=(\pi,\pi)$. The leading-order effect of the spin fluctuations on the fermionic spectrum at zero temperature is given by the one-loop contribution to the self-energy in Fig. 1.

$$\Sigma_0(\mathbf{k},\omega)=-\tfrac{3}{2}iU^2\frac{1}{N}\sum_{\mathbf{q}}\int\frac{d\nu}{2\pi}\chi(\mathbf{q},\nu)G_0(\mathbf{k}-\mathbf{q},\omega-\nu)\ .$$
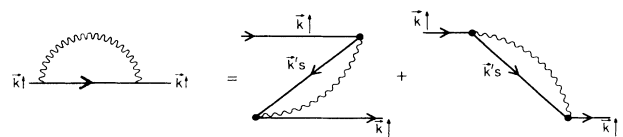
$$(2)$$

FIG. 1. Leading-order contribution to the self-energy from AF spin fluctuations and its two time-ordered Feynman diagram components.

Here, $G_0(\mathbf{k},\omega)$ is the single-particle propagator in the absence of interactions and U is the on-site Coulomb energy of the repulsive Hubbard model. Since we use a phenomenological susceptibility as input, the Hubbard U will be absorbed into an effective coupling constant. To this order all single-particle properties then follow from the propagator

$$G_1(\mathbf{k},\omega)=[\omega-\varepsilon(\mathbf{k})-\Sigma_0(\mathbf{k},\omega)]^{-1} , \tag{3}$$

$\varepsilon(\mathbf{k})$ is the dispersion of the noninteracting tight-binding band

$$\varepsilon(\mathbf{k})=-2t[\cos(k_x a)+\cos(k_y a)] \tag{4}$$

that models the partially filled antibonding band of the CuO_2 planes with an effective hopping matrix element t and lattice constant a.

II. MODEL SUSCEPTIBILITY

The model susceptibility[1] that we will consider in (2) is given by

$$\chi(\mathbf{q},\omega)=-\lambda^2 a^2(\Gamma)\sum_{\mathbf{Q}=(\pm\pi,\pm\pi)}\frac{\Gamma}{(q_x-Q_x)^2+\Gamma^2}\frac{\Gamma}{(q_y-Q_y)^2+\Gamma^2}\int g(\nu)\frac{2\nu}{\omega^2-\nu^2+i\delta}d\nu \tag{5}$$

The enhancement of the susceptibility at the AF wave vectors $\mathbf{Q}$ is simply represented by the Lorentzians centered at the four corners of the Brillouin zone, which are normalized to unity by a $(\Gamma)=\pi/\arctan(2\pi/\Gamma)$. The inverse of their width Γ is a measure of the spin-spin correlation length and λ is a coupling constant, whose value is determined below.

The frequency dependence of χ is not crucially important for the purpose of our analysis. Since we are focusing on the paramagnetic phase with only short-range spin correlations it is reasonable that the spin fluctuations can be modeled by a distribution of dispersionless propagating bosons. For simplicity we chose the frequency distribution $g(\omega)$ to be linear up to a cutoff ω_0 that determines the characteristic scale for spin fluctuations

$$g(\omega)=\frac{2}{\omega_0}\frac{\omega}{\omega_0}\Theta(\omega-\omega_0) . \tag{6}$$

Since ω_0 is small compared to the SDW energy gap (of order the Hubbard U) that opens up at half-filling[6] the results of our analysis are not sensitive to the detailed form of $g(\omega)$. Qualitatively similar results are obtained for a phenomenological susceptibility[7] that has been used to explain and fit the data from NMR and NQR experiments or for a form of the susceptibility that has been used to fit the data from neutron scattering experiments.[3] Results from a random-phase-approximation (RPA) calculation are planned to be presented elsewhere.[8]

For our model susceptibility it is instructive to evaluate first the simple static limit $g(\omega)=\delta(\omega)$ at half-filling ($\mu=0$), with an infinite spin-spin correlation length corresponding to $\Gamma=0$. In this limit the susceptibility reduces to four δ functions at the corners of the Brillouin zone, i.e.,

$$\chi(\mathbf{q},\omega)=i\pi\lambda^2\delta(\omega)\tfrac{1}{4}\sum_{\mathbf{Q}=(\pm\pi,\pm\pi)}\delta(\mathbf{q}-\mathbf{Q}) . \tag{7}$$

The corresponding self-energy in this limit is given by

$$\Sigma_0(\mathbf{k},\omega)=\frac{1}{2}\frac{(\lambda U)^2}{\omega+\varepsilon(\mathbf{k})+i\delta\mathrm{sgn}[\varepsilon(\mathbf{k})]} . \tag{8}$$

Solving for the poles of $G_1(\mathbf{k},\omega)$ we find the two quasiparticle bands $E(\mathbf{k})=\pm[\varepsilon^2(\mathbf{k})+\Delta^2]^{1/2}$ split by the gap $\Delta=(\tfrac{1}{2})^{1/2}\lambda U$, reflecting the broken symmetry of the antiferromagnetic insulator. Correspondingly, the spectral function

$$A(\mathbf{k},\omega-\mu)=(1/\pi)|\mathrm{Im}G_1(\mathbf{k},\omega)| \tag{9}$$

has two δ-function contributions

$$A(\mathbf{k},\omega)=\tfrac{1}{2}\left[1+\frac{\varepsilon(\mathbf{k})}{E(\mathbf{k})}\right]\delta(\omega-E(\mathbf{k}))$$

$$+\tfrac{1}{2}\left[1-\frac{\varepsilon(\mathbf{k})}{E(\mathbf{k})}\right]\delta(\omega+E(\mathbf{k})) \tag{10}$$

for the upper and lower SDW or Mott-Hubbard bands, respectively. The result for the gap can in fact also be used to adjust the coupling constant λ in order to match the result from the gap equation

$$\frac{1}{U}=\sum_{\mathbf{k}}'\frac{1}{\sqrt{\varepsilon(\mathbf{k})^2+\Delta^2}} \tag{11}$$

that is obtained by a self-consistent Hartree-Fock calculation in the presence of the SDW.[6] The prime on the momentum sum indicates that the summation is restricted to the magnetic Brillouin zone, e.g., for $U=4t$ we find $\lambda=0.2$.

III. SPECTRAL FUNCTION AND PSEUDOGAP

To investigate the interesting regime where the spin-spin correlation length is of order of 3–4 lattice spacings we have to evaluate the self-energy (2) numerically even for the simple model susceptibility that we chose. We separately evaluate the spectral functions for weak and moderate hole doping, depending on whether the position of the chemical potential satisfies either (a) $-\Delta<\mu<0$ or (b) $\mu<-\Delta$, where Δ is the value of the SDW gap that we obtain in the limit $\Gamma\to0$ as discussed above. For the intermediate regime there will be no true gap in the single-particle spectrum but instead a pseudogap will be present that sharpens as we approach the antiferromagnetic insulator.

Figure 2 shows the evolution of the spectral function with increasing spin-spin correlation length for $\mu \approx -0.3\Delta$ corresponding to a hole doping concentration δ less than about 8%. For $\Gamma=1.0$ the susceptibility $\chi(\mathbf{q},\omega)$ is almost flat in $\mathbf{q}$ and AF correlations play essentially no role. This is the usual situation for a conventional Fermi-liquid metal, and as in Fig. 2(a) the spectral function is dominated by a single-quasiparticle peak plus an incoherent background from the particle and hole continua. With decreasing Γ the quasiparticle peak looses spectral weight to the incoherent pieces that begin to dominate the spectral function [Figs. 2(b) and 2(c)]. Two broad peaks develop, separated approximately by $2\Delta=2\lambda U/2^{1/2}$ as the precursors of the upper and lower SDW bands. Nevertheless, the quasiparticle at the chemical potential persists for all finite values of Γ and its spectral weight, as determined by the quasiparticle residue

$$z_{\mathbf{k}} = \cfrac{1}{1 - \cfrac{\partial\Sigma(\mathbf{k},\omega)}{\partial\omega}\bigg|_{\omega=\mu}} \qquad (12)$$

remains finite but becomes very small for longer-range spin correlations. For a correlation length of about 20 lattice spacings the quasiparticle peak carries only 1% of the total spectral weight. It is in this sense that the system remains a Fermi liquid, although its properties are far from conventional, as becomes most obvious from the spectral functions in Fig. 2. In particular, while the system may respond at long wavelengths and low frequencies as a Fermi liquid, the typical wavelength involved in pairing in high-T_c materials is $\xi_0 \approx 12$ Å in the a-b plane.[9] Also, the typical pairing frequencies are of order the spin-wave energy $J \approx 1200$ K.[10] Thus, the quasiparticles are not well defined in the regions they are required and an alternative approach to constructing a pairing theory must be developed.

The shift of spectral weight to the incoherent parts of $A(\mathbf{k},\omega)$ can be best understood by splitting the one-loop Feynman diagram for the self-energy into its two time-ordered components as in Fig. 1. The forward scattering (in time) diagram describes the conventional dressing of the particle and may be referred to as the magnetic polaron contribution. The backward-scattering (in time) dia-
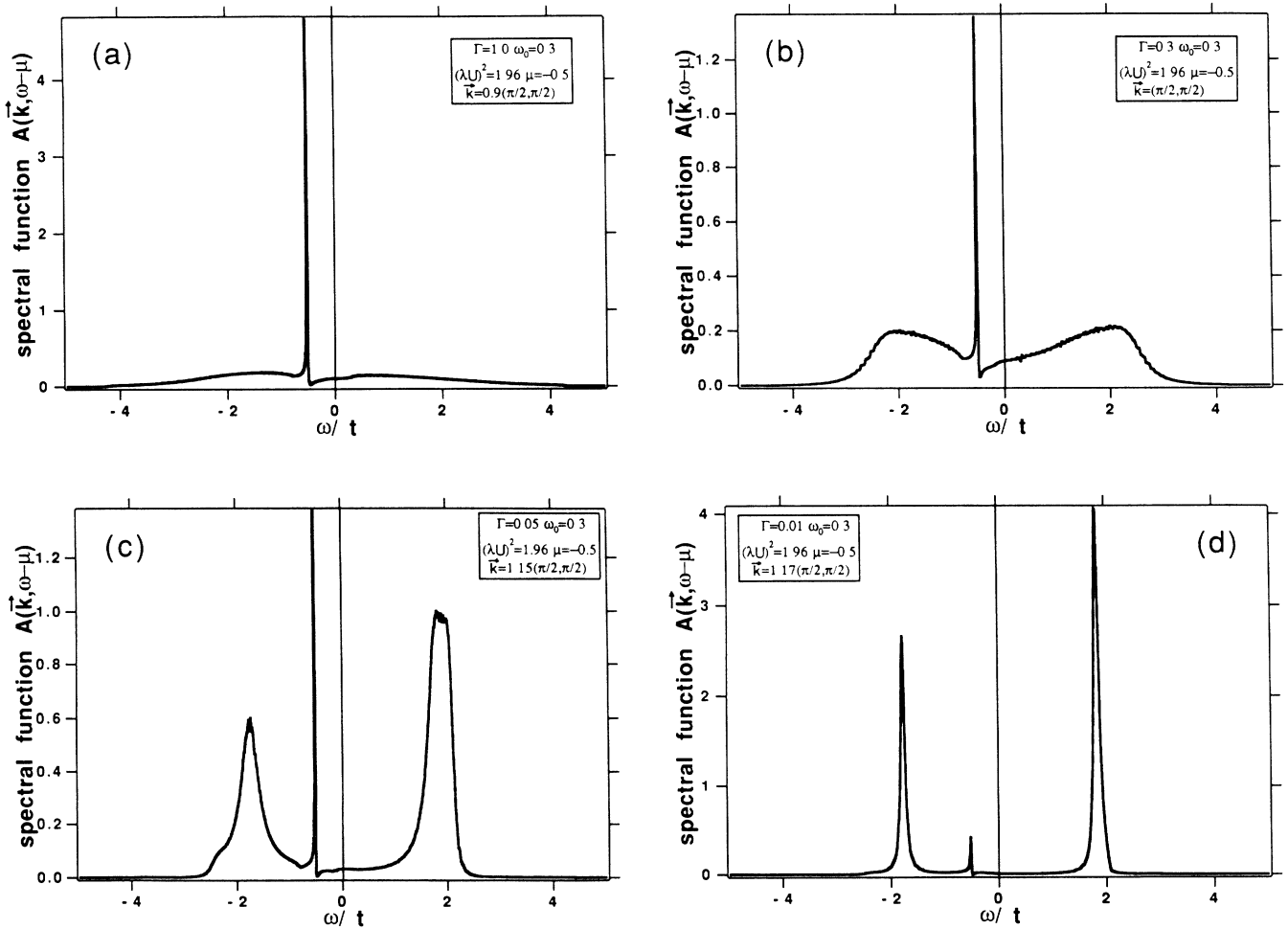

FIG. 2. Evolution of the spectral function $A(\mathbf{k},\omega)$ with increasing spin-spin correlation length for $(\lambda U)^2=1.96$, $\mu=-0.5\approx-0.3\Delta_{\mathrm{SDW}}$, and momenta $\mathbf{k}$ close to $\mathbf{k}_f$. (a) $\Gamma=1.0$; (b) $\Gamma=0.3$; (c) $\Gamma=0.05$; (d) $\Gamma=0.01$. Energies are measured in units of t.

gram involves an intermediate state with a hole below the Fermi surface and two electrons in the same momentum and spin state above the Fermi surface. This Pauli-principle-violating diagram exactly cancels a vacuum fluctuation diagram, with a particle in the same momentum and spin state as the added particle. Thus, this vacuum fluctuation is suppressed. Since vacuum fluctuations lower the energy of the system, their suppression increases the energy, and hence, the self-energy contribution from the backward-scattering diagram is positive for particles (and negative for holes). We note that this is also the origin of the spin-bag pairing attraction, since particles can mutually reduce their positive self-energy contributions from spin fluctuations, as represented by a crossed line diagram in the particle-particle channel as discussed in Ref. 1.

The qualitative behavior $\Sigma(\mathbf{k},\omega)$ is indicated in Fig. 3. In the conventional Fermi-liquid regime [Fig. 3(a)] Σ is essentially $\mathbf{k}$ independent and we find one solution of $\omega-\varepsilon(\mathbf{k})-\text{Re}\Sigma(\mathbf{k},\omega)=0$ leading to a single-quasiparticle peak in $A(\mathbf{k},\omega)$. In the pseudogap regime with finite range AF spin correlations the suppression of vacuum fluctuations becomes important, as described above, and the real part of Σ has now a large positive (negative) contribution for particles (holes) from the "backward-scattering" diagram in Fig. 1. This change in the self-energy then leads to five solutions of $\omega-\varepsilon(\mathbf{k})-\text{Re}\Sigma(\mathbf{k},\omega)=0$, as indicated in Fig. 3(b). Although there is a sharp crossover from a situation with one quasiparticle solution to (three and) five solutions of $\omega-\varepsilon(\mathbf{k})-\text{Re}\Sigma(\mathbf{k},\omega)=0$, the spectral function still changes smoothly due to the presence of the imaginary part of Σ. In Fig. 3(b) the solutions 1 and 5 correspond
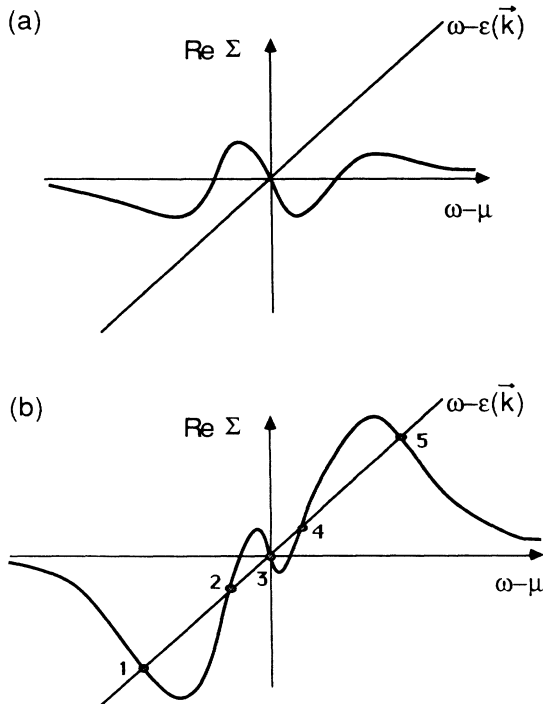

FIG. 3. Qualitative behavior of the real part of the self-energy in the (a) Fermi liquid and the (b) pseudogap regime.

to the developing upper and lower SDW bands, solution 3 still describes the quasiparticle that was present in the weakly correlated Fermi liquid limit in Fig. 3(a). The solutions 2 and 4 are accompanied by a large imaginary part of Σ and contribute only to the incoherent background of the spectral function.

Near half-filling the Fermi surface is almost perfectly nested, and most scattering events with momentum transfer close to $\mathbf{Q}$ will scatter an electron injected above the Fermi surface to below the Fermi surface. Furthermore, if a vacuum fluctuation hole is present, due to the strong enhancement of the susceptibility around $\mathbf{Q}$ these processes tend to dominate, leading to the dominance of the self-energy diagram with the backward propagating intermediate line.

The shift of spectral weight to the incoherent parts of $A(\mathbf{k},\omega)$ is responsible for the formation of the pseudogap in the density of states per spin as given by the momentum space average of the spectral function

$$N(\omega)=\frac{1}{N}\sum_{\mathbf{k}} A(\mathbf{k},\omega) .$$ (13)

For a fixed value of μ the hole doping δ is then determined by integrating the density of states up to the chemical potential

$$1-\delta=2\int_{-\infty}^{\mu} N(\omega)d\omega .$$ (14)

As shown in Fig. 4 the pseudogap develops around $\omega=0$, which is the position of the chemical potential at half-filling. If at finite hole doping the short-range spin order is incommensurate, i.e., if the peak in $\chi(\mathbf{q},\omega)$ is shifted to $\mathbf{Q}^{*}=\mathbf{Q}-\Delta\mathbf{q}\sim 2\mathbf{k}_f$, where $\mathbf{k}_f$ is the Fermi momentum of the noninteracting $U=0$ case, the center of the pseudogap will move downward to the position of μ. For larger hole doping concentrations the pseudogap is less well developed.

It is important to note that for nearly commensurate spin order, the pseudogap is still centered around $\omega=0$, while the chemical potential moves downward into a region with a large density of states. Thus, instead of having a small density of states at the Fermi energy, the pseudogap formulation leads to a large density of states for moderate doping levels. This is consistent with a static susceptibility that grows with hole doping as seen in experiment.[11]

Figure 5 shows the evolution of the spectral function for the case where $\mu < -\Delta$. Here, the Fermi momentum along the diagonal of the Brillouin zone was fixed to $\mathbf{k}_f=0.9(\pi/2,\pi/2)$ and the spectral functions are plotted as a function of ω for fixed momentum $\mathbf{k}=0.95(\pi/2,\pi/2)$ above $\mathbf{k}_f$. The position of the chemical potential $\mu < -\Delta$ corresponds to a larger hole doping concentration δ, as in Fig. 2, and for the parameters chosen δ is about 20%. In this case the quasiparticle peak of the Fermi-liquid regime evolves into the renormalized quasiparticle within the lower SDW band. In addition, a second peak is formed out of the incoherent particle background, which evolves into the coherent quasiparticle of the upper SDW band.

IV. PHOTOEMISSION
AND INVERSE PHOTOEMISSION

The formation of the upper and lower SDW bands in the crossover regime with finite-range spin correlations should be observable by angle-resolved (AR) photoemission and inverse photoemission spectroscopy. These ex-

periments directly measure the spectral function $A(\mathbf{k}, \omega - \mu)$ multiplied by a thermal Fermi factor. In the Fermi-liquid regime the quasiparticle peak of $A(\mathbf{k}, \omega)$ defines a single energy $E(\mathbf{k})$ for each value of $\mathbf{k}$ in the first Brillouin zone, as sketched along the diagonal $\mathbf{k} = (k_x, k_x)$ in Fig. 6(a).

When an SDW is present, $\mathbf{k}$ is mixed with $\mathbf{k} + \mathbf{Q}$ by ex-
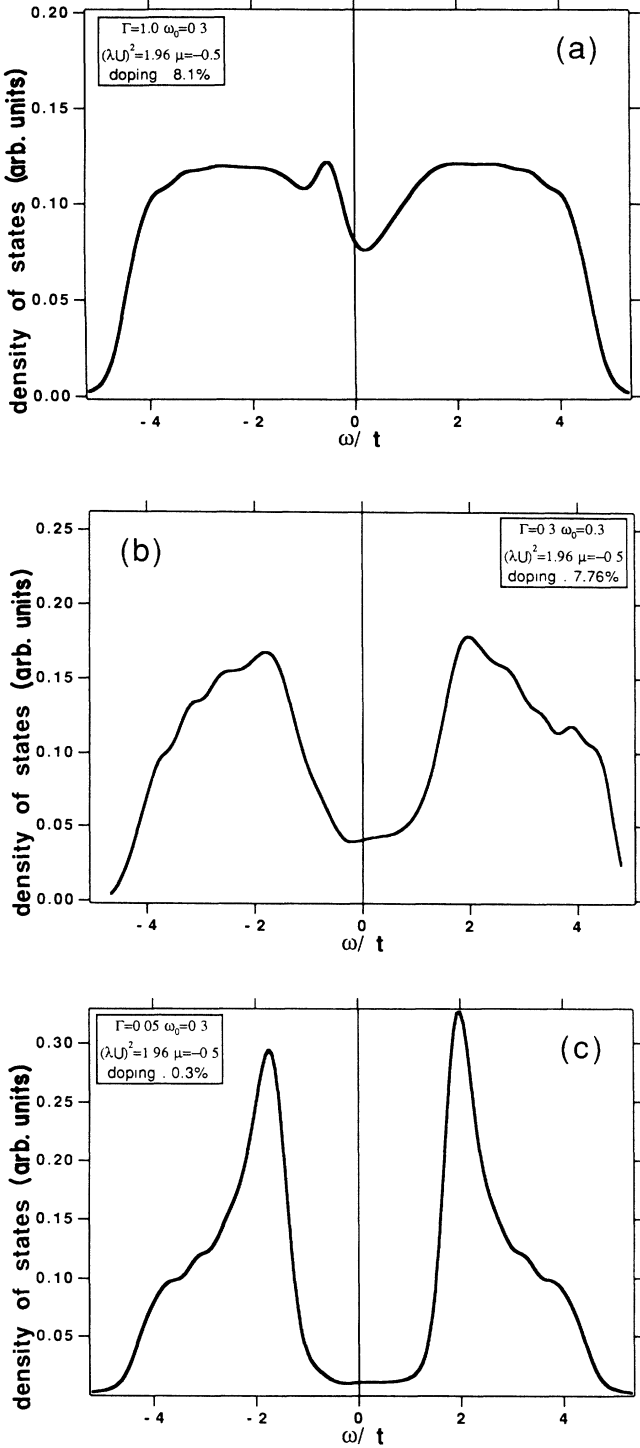

FIG. 4. Evolution of the density of states with increasing correlation length for $\mu = -0.5$. (a) $\Gamma = 1.0$; (b) $\Gamma = 0.3$; (c) $\Gamma = 0.05$.
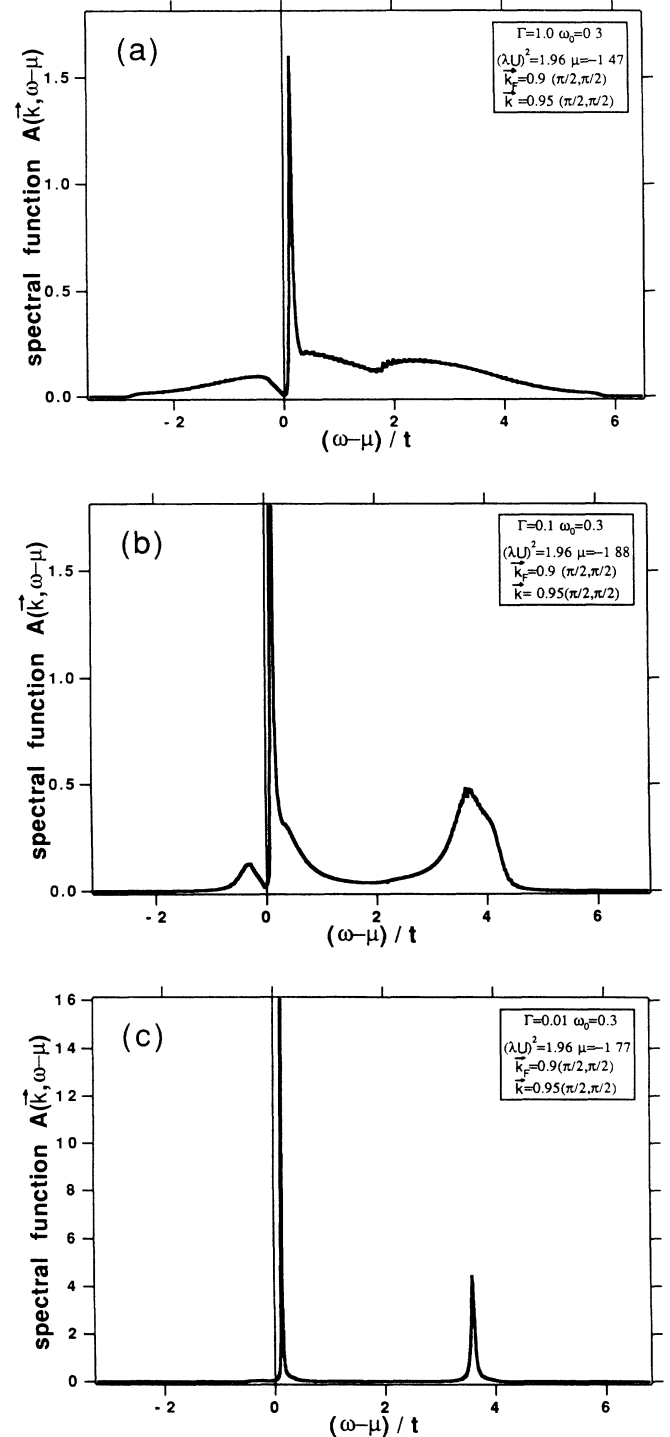
FIG. 5. Evolution of the spectral function $A(\mathbf{k}, \omega)$ for $\mu < -\Delta$. (a) $\Gamma = 1.0$, (b) $\Gamma = 0.3$, (c) $\Gamma = 0.01$.

change Bragg scattering, such that the energy eigenstates $|\phi_{\mathbf{ks}}\rangle$ no longer have a sharp momentum,

$$|\phi_{\mathbf{ks}}\rangle = u_{\mathbf{k}}|\mathbf{k}\rangle + s v_{\mathbf{k}}|\mathbf{k}+\mathbf{Q}\rangle, \quad u_{\mathbf{k}}^2 + v_{\mathbf{k}}^2 = 1 .$$

The energy spectrum of the $|\phi_{\mathbf{ks}}\rangle$ states is shown in Fig. 6(b), where the states denoted by a heavy line carry large
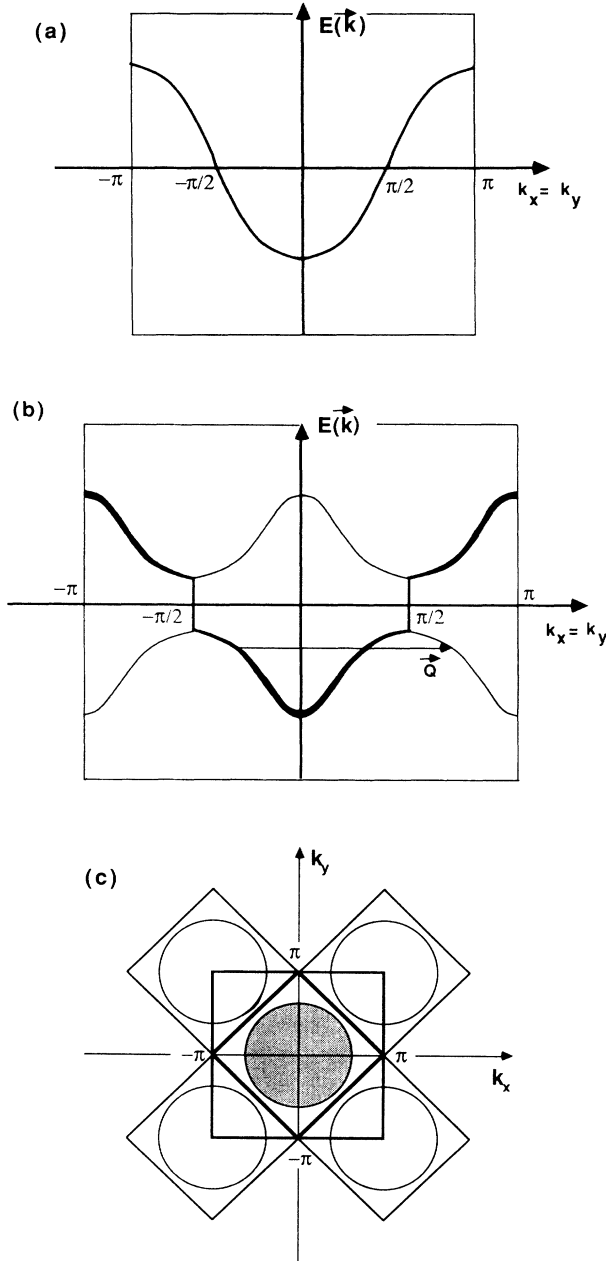

(a)

(b)

(c)

FIG. 6. (a) Single-quasiparticle band $E(\mathbf{k})$ in the Fermi-liquid regime along the diagonal of the first Brillouin zone. (b) Quasiparticle (heavy line) and shadow band (light line). (c) Fermi sea and its mirror images in the second magnetic zones. The large square represents the first Brillouin zone and the smaller squares represent the first and second magnetic zones, respectively.

weight $u_{\mathbf{k}}^2 > \frac{1}{2}$ and the states denoted by a light line carry a small weight $v_{\mathbf{k}}^2 < \frac{1}{2}$. Thus, if one creates a hole of energy $E(\mathbf{k})$ in the lower band by photoemission, one will observe the emitted electron having momenta $\mathbf{k}$ with probability $u_{\mathbf{k}}^2$ and $\mathbf{k}+\mathbf{Q}$ with probability $1-u_{\mathbf{k}}^2$. Hence, the Bragg scattering leads to a "shadow band" displaced by $\mathbf{Q}$ as shown in Fig. 6(c).

If the AF spin-correlation length is finite, these effects persist with $\mathbf{Q}$ being replaced by a sum over $\mathbf{q}\sim\mathbf{Q}$. Furthermore, the same effects occur for the upper band and the unoccupied part of the lower band, and should be seen in angle-resolved (AR) inverse photoemission spectra. We note that $u_{\mathbf{k}}^2 \approx v_{\mathbf{k}}^2 \approx \frac{1}{2}$ near the edge of the pseudogap $\pm\Delta$, while the intensity $v_{\mathbf{k}}^2$ of the shadow band decreases strongly for energies greater than $\pm 2\Delta$ from the gap center.

V. FINITE TEMPERATURES

A separate issue that can be addressed is the line shape and width of the quasiparticle peak that is observed in AR photoemission experiments.[12] For the purpose of a qualitative comparison, we extend our analysis to finite temperatures and introduce the temperature Green's function

$$\overline{G}(\mathbf{k},z) = \frac{1}{z - \varepsilon(\mathbf{k}) + \mu - \overline{\Sigma}(\mathbf{k},z)} . \tag{15}$$

The corresponding self-energy is to one-loop order evaluated at the discrete set of fermionic Matsubara frequencies $i\omega_n = i(2n+1)\pi/\beta$. β is the inverse of the temperature, $\beta = 1/k_B T$. $\overline{\Sigma}$ is given by[13]

$$\overline{\Sigma}(\mathbf{k},i\omega_n) = \frac{3}{2}U^2 \frac{1}{N}\sum_{\mathbf{q}}\int_0^\infty \frac{d\omega}{\pi} \mathrm{Im}\chi(\mathbf{q},\omega)$$

$$\times \left[\frac{1 - f_{\mathbf{k}-\mathbf{q}} + n(\omega)}{i\omega_n - \varepsilon_{\mathbf{k}-\mathbf{q}} + \mu - \omega} \right.$$

$$\left. + \frac{f_{\mathbf{k}-\mathbf{q}} + n(\omega)}{i\omega_n - \varepsilon_{\mathbf{k}-\mathbf{q}} + \mu + \omega} \right] , \tag{16}$$

where $f_{\mathbf{k}-\mathbf{q}} \equiv f(\varepsilon_{\mathbf{k}-\mathbf{q}} - \mu)$ and $n(\omega)$ denote the Fermi and Bose functions, respectively. The spectral function $A(\mathbf{k},\omega)$ is determined by the discontinuity of the Green's function across the real axis and is given by

$$A(\mathbf{k},\omega-\mu) = \frac{1}{\pi} \frac{\Gamma(\mathbf{k},\omega)}{[\omega - \varepsilon(\mathbf{k}) - \mathrm{Re}\Sigma(\mathbf{k},\omega)]^2 + \Gamma(\mathbf{k},\omega)^2} , \tag{17}$$

where the quasiparticle lifetime $\Gamma(\mathbf{k},\omega)$ is determined by the imaginary part of the self-energy,

$$\mathrm{Im}\overline{\Sigma}(\mathbf{k},\omega-\mu) = -\mathrm{sgn}(\omega-\mu)\Gamma(\mathbf{k},\omega) . \tag{18}$$

AR photoemission experiments measure $A(\mathbf{k},\omega-\mu)f(\omega-\mu)$. Ideally, in the photoemission process the momentum parallel to the surface is conserved when the photoelectron leaves the crystal. Aligning the crystal surface parallel to the CuO_2 planes therefore allows one
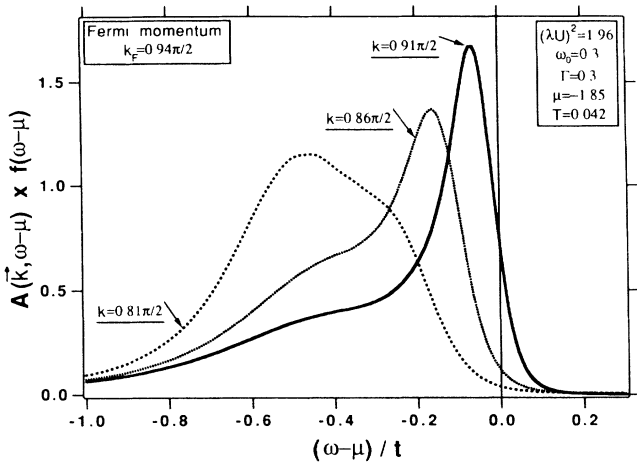
FIG. 7. Angular-resolved photoemission spectra for momenta along the diagonal of the Brillouin zone $k_x = k_y \equiv k$ close to the Fermi momentum k_f.

to directly determine the initial in-plane momentum state.[12] Using the phenomenological model susceptibility we can evaluate $A(\mathbf{k},\omega)$ for different momenta close to the Fermi momentum k_f for a moderate spin-spin correlation length of about three to four lattice spacings. Figure 7 shows the corresponding photoemission signals as the quasiparticle peak disperses through the Fermi level. The line shape that arises within our treatment may be compared with the experimental data by Olson et al.[12] after subtracting the background contribution from secondary photoelectrons. The predicted line shape is very similar to the experimental results. The experimental data therefore do not unambiguously require the presence of a cusplike singularity, as recently suggested by Anderson[14] in the context of a Luttinger liquid description of the normal-state properties of cuprate superconductors. Rather, the available data are consistent with an interpretation in terms of a Fermi-liquid based theory of a highly correlated metal.[15]

The experimental AR photoemission data have been fitted by a series of equally spaced Lorentzians with a k-independent width scaling linearly with binding energy. However, the finite angular acceptance of the spectrometer already leads to an energy broadening of about 100 meV.[16] Despite the high resolution achieved so far, the photoemission experiments therefore cannot reveal any information about the quasiparticle lifetime or ImΣ within an energy range of ~ 1000 K around the Fermi level. Hence, the present photoemission data cannot serve as a test for any theoretical concept addressing the low-energy physics.

VI. CONCLUSION AND SUMMARY

In this paper we have shown how antiferromagnetic spin fluctuations lead to qualitative changes in the spectral function of a metallic system. Spectral weight is shifted from the quasiparticle peak of the conventional Fermi-liquid metal to the incoherent particle and hole backgrounds that develop into sharp coherent peaks with

increasing spin-spin correlation length. These peaks can be viewed as the precursors of the valence and conduction band of the antiferromagnetic insulator that are folded back into the magnetic zone when long-range spin order sets in.

The antiferromagnetic fluctuations lead to a pseudogap in the density of states that sharpens to become the SDW exchange gap as the system becomes antiferromagnetically ordered. The origin of the pseudogap and the changes in the spectral function arise from the backward-scattering diagram contribution to the self-energy that describes the exchange suppression of vacuum fluctuations that lower the ground-state energy in the absence of an added carrier and hence raise the energy to insert a particle or a hole. This effect dominates over the polaronlike effect if the Fermi surface is close to nesting and the spin susceptibility is strongly peaked close to the AF wave vector $\mathbf{Q}$, favoring scattering events with large momentum transfer.

While the SDW approach discussed above is appropriate for weak coupling, local-moment formation becomes important for large U, leading to a Mott-Hubbard gap whose characteristic energy $2\Delta_{MH}$ is independent of spin order on neighboring sites. While this gap is frequently referred to as a charge gap,[14,17] it can equally well be viewed in a one-band model as arising from the exchange interaction of the added electron or hole, with the local moment as follows from the identity

$$U n_{i\uparrow} n_{i\downarrow} = \frac{U}{2}(n_{i\uparrow} + n_{i\downarrow})^2 - \frac{U}{2}(n_{i\uparrow} + n_{i\downarrow})$$

$$= -\frac{U}{2}(n_{i\uparrow} - n_{i\downarrow})^2 + \frac{U}{2}(n_{i\uparrow} + n_{i\downarrow}) . \quad (19)$$

In this limit, multiple-scattering diagrams must be included to take account of both, the on-site spin order and the suppression of local AF order surrounding the added particle, as discussed above. We are currently studying how local moments and local AF order can be simultaneously included within a diagram approach.

Angle-resolved photoemission experiments provide a direct test of the presence of the "shadow bands". Thus far such experiments performed on the cuprate superconductors in the normal state have focused on mapping out the Fermi surface, following the position of the quasiparticle peak for different momenta $\mathbf{k}$ until it disperses through the Fermi surface at k_f. For sufficiently strong AF spin fluctuations its mirror image will show up at the same binding energy at a momentum $\mathbf{k}+\mathbf{Q}$. In addition, AR inverse photoemission experiments can in principle detect the same effects for the unoccupied parts of the lower and the upper band.

ACKNOWLEDGMENTS

*Permanent address: Department of Physics, University of California, Santa Barbara, California 93106.

[1]A. Kampf and J. R. Schrieffer, Phys. Rev. B 41, 6399 (1990).

[2]G. Shirane, R. J. Birgeneau, Y. Endoh, P. Gehring, M. A. Kastner, K. Kitazawa, H. Kojima, I. Tanaka, T. R. Thurston, and K. Yamada, Phys. Rev. Lett. 63, 330 (1989).

[3]J. M. Tranquada, W. J. L. Buyers, H. Chou, T. E. Mason, M. Sato, S. Samoto, and G. Shirane, Phys. Rev. Lett. 64, 800 (1990).

[4]R. E. Walstedt, W. W. Warren, Jr., R. F. Bell, G. F. Brennert, G. P. Espinosa, R. J. Cava, L. F. Schneemeyer, and J. V. Waszak, Phys. Rev. B 38, 9299 (1988); P. C. Hammel, M. Takigawa, R. H. Heffner, Z. Fisk, and K. Ott, Phys. Rev. Lett. 63, 1992 (1989).

[5]T. R. Thurston, R. J. Birgeneau, M. A. Kastner, N. W. Preyer, G. Shirane, Y. Fujii, K. Yamada, Y. Endoh, K. Kakurai, M. Matsuda, Y. Hidaka, and T. Murakami, Phys. Rev. B 40, 4585 (1989); for a review see, e.g., R. J. Birgeneau, in *Physical Properties of High Temperature Superconductors II*, edited by D. M. Ginsberg (World Scientific, Singapore, 1990).

[6]J. R. Schrieffer, X. G. Wen, and S. C. Zhang, Phys. Rev. B 39, 11 663 (1989).

[7]A. J. Millis, H. Monien, and D. Pines, Phys. Rev. B 42, 167 (1990).

[8]A. Kampf (unpublished).

[9]U. Welp, W. K. Kwok, G. W. Crabtree, K. G. Vandervoort, and J. Z. Liv, Phys. Rev. Lett. 62, 1908 (1989).

[10]T. Thio, T. R. Thurston, N. W. Preyer, P. J. Picone, M. A. Kastner, H. P. Jenssen, D. R. Gabbe, C. Y. Chen, R. J. Birgeneau, and A. Aharony, Phys. Rev. B 38, 905 (1988); T. Becher and G. Reiter, Phys. Rev. Lett. 63, 1004 (1989).

[11]D. C. Johnston, S. K. Sinha, A. J. Jacobson, and J. M. Newson, Physica B + C 153-155C, 572 (1988).

[12]C. G. Olson, R. Liu, D. W. Lynch, R. S. List, A. J. Arko, B. W. Veal, Y. C. Chang, P. Z. Jiang, and A. P. Paulikas, Phys. Rev. B 42, 381 (1990); Science 245, 731 (1989).

[13]N. F. Berk and J. R. Schrieffer, Phys. Rev. Lett. 17, 433 (1966); S. Doniach and S. Engelsberg, *ibid.* 17, 750 (1966); W. Brinkman and S. Engelsberg, Phys. Rev. B 169, 417 (1968).

[14]P. W. Anderson and Y. Ren, in *High Temperature Superconductivity: The Los Alamos Symposium-1989*, edited by K. S. Bedell, D. Coffey, D. E. Meltzer, D. Pines, and J. R. Schrieffer (Addison-Wesley, Redwood City, 1990).

[15]Similar results have been reported by H. Kim and P. S. Riseborough (unpublished); see also P. S. Riseborough, Phys. Rev. B 40, 8131 (1989).

[16]A. Arko and S. List (private communication).

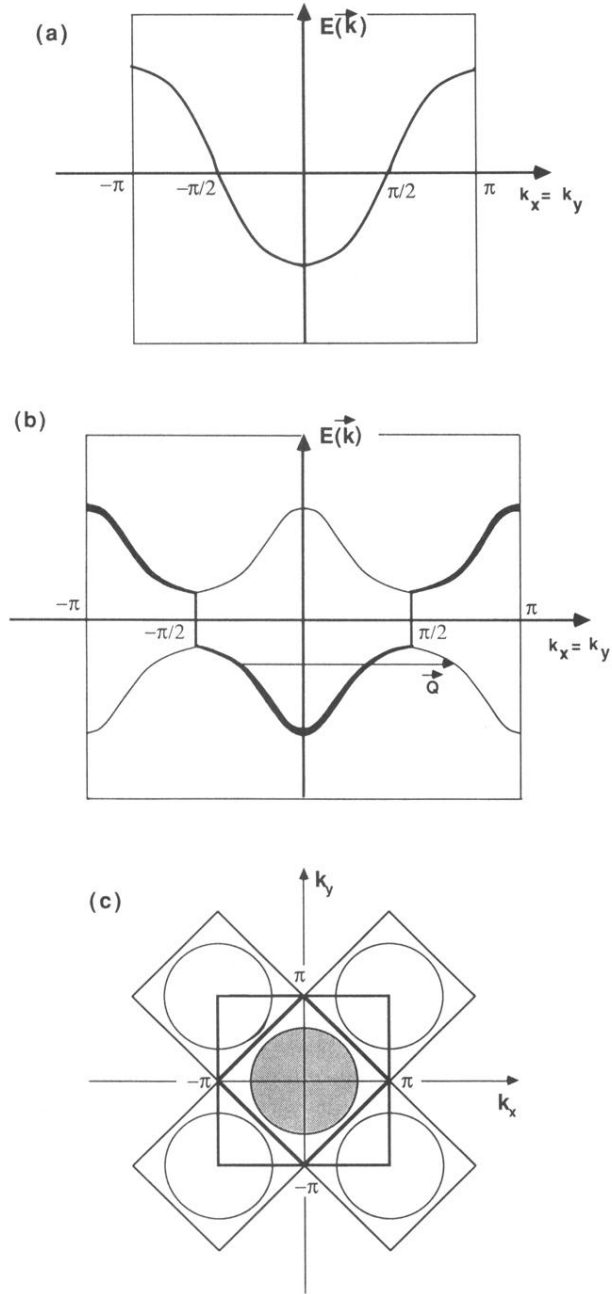[17]C. A. R. Sa de Melo and S. Doniach, Phys. Rev. B 41, 6633 (1990).

FIG. 6. (a) Single-quasiparticle band $E(\mathbf{k})$ in the Fermi-liquid regime along the diagonal of the first Brillouin zone. (b) Quasiparticle (heavy line) and shadow band (light line). (c) Fermi sea and its mirror images in the second magnetic zones. The large square represents the first Brillouin zone and the smaller squares represent the first and second magnetic zones, respectively.